Mozammel Mazumder
Qiang Xu*

Modeling and Optimization for a Comprehensive Gas Processing Plant with Sensitivity Analysis and Economic Evaluation

Sweetening, dehydration, natural gas liquid (NGL) recovery, and sale gas compression are four major treatment stages for the general natural gas processing. Here, a comprehensive gas processing plant (CGPP) coupling sweetening, dehydration, NGL recovery, and compression subsystems have been conceptually designed, modeled, and optimized based on field data. The development includes four major stages of work: (i) CGPP process development with Aspen HYSYS simulator; (ii) sensitivity studies for all distillation columns involved in the CGPP process to optimize their performances; (iii) sizing of major equipment of the CGPP; and (iv) economic evaluations with Aspen process economic analyzer to calculate the expected capital and operating expenditures for the developed CGPP process. Valuable insights of natural gas monetization from the viewpoint of large-scale process system integration, modeling, and optimization are provided.

Keywords: Comprehensive gas processing plant, Dehydration, Natural gas liquid, Natural gas processing

Received: July 02, 2020; *revised:* July 26, 2020; *accepted:* August 13, 2020

DOI: 10.1002/ceat.202000216

Supporting Information available online

1 Introduction

Among all fossil fuels, natural gas will become a major clean energy resource worldwide in the coming decades. Natural gas has been widely used as the feedstock and fuel gas in the chemical and petrochemical industries [1]. Its treatment units are designed based on the impurities present in the raw natural gas and permissible limits of these impurities in the sales gas. Typically, those specifications include water content, hydrocarbon dew point, heating value, carbon dioxide and hydrogen sulfide removal [2–4]. Thus, processes required to meet sales gas specifications usually include dehydration, sweetening (removal of H_2S and CO_2), compression, and hydrocarbon dew point control [5]. A typical block flow diagram for a general natural gas treatment plant is presented in Fig. S1 in the Supplementary Information.

Generally, after the raw natural gas is collected, all acid gases like H_2S and CO_2 shall be removed first from the natural gas feed to prevent corrosive damage to the downstream equipment and piping [6]. The feed gas compositions and conditions, desired purity of the treated gas, and the selectivity of H_2S over CO_2 act as the evaluation criteria of acid gas removal technologies. The acid gas flows to the gas sweetening unit (GSU), also called acid gas removal unit (AGRU), where H_2S and CO_2 will be removed. Methyldiethanolamine (MDEA) is a tertiary amine that offers many advantages over other alkanol amines [7]. The difference in the reaction rates with H_2S and CO_2 gives MDEA a desirable feature over other amines, namely, selectivity of H_2S over CO_2. H_2S is removed by an amine solvent to meet the total sulfur product specification, typically 4 ppmv. CO_2 is removed to 50 ppmv to avoid CO_2 freezing in the main exchangers in the liquefaction plant [8]. Diethanol amine (DEA) is widely used in the industry due to its lower heats of reaction, higher acid gas carrying capacity, and resultant lower energy requirements, while avoiding the significant problems of corrosion and solvent degradation. DEA could also have potential for selective H_2S removal from streams containing CO_2 under certain conditions [9–11]. For the above reasons, DEA was chosen for the gas sweeting unit in this paper.

The presence of water vapor in the gas stream poses serious problems such as plugging, pipeline corrosion, reduction of line capacity, and reduction of combustion efficiency [12]. Formally, the process of water removal from a natural gas stream is called the gas dehydration process. It includes glycol absorption, polymer membranes, composite membranes, molecular sieves, and isenthalpic gas cooling with controlled hydrate formation [13–16]. Glycol absorption is the dehydration method

Mozammel Mazumder, Prof. Qiang Xu
Qiang.xu@lamar.edu
Dan F. Smith Department of Chemical Engineering, Lamar University, Beaumont, TX, 77710, USA.

used in the majority of existing natural gas treatments plants. The commonly available glycols are monoethylene glycol (MEG), diethylene glycol (DEG), triethylene glycol (TEG), and tetraethylene glycol (TREG) [17]. TEG is the most commonly used solvent for natural gas dehydration since its adsorption dehydration can achieve very low water content and is best applied to where a very low dew point is required. It has high hygroscopicity and low solubility in natural gas and low vapor pressure. MEG and DEG can also be taken for dehydration applications. However, their performance in terms of solvent loss and thermal degradation in the regeneration system are normally poorer than those from TEG [18, 19].

After 1970, some changes were carried out on conventional glycol units for raising glycol concentration. These changes include using a stripping gas column after the regeneration reboiler [20]. In 1970, the Dow chemical company presented a process in which volatile materials were used to increase water volatility in the regeneration unit. These processes were called Drizo and Super Drizo [21, 22]. In 1993, by utilizing this process, a glycol concentration of 99.99 wt % was achieved [23, 24]. There are also many commercially available processes for customized dehydration systems, especially absorption in TEG [25].

After dehydration, the natural gas liquid (NGL) should be removed to maintain the natural gas dew point as well as yield a source of revenue from NGL [26]. Actually, NGL has a significantly greater value than the main product of methane. The lighter NGL fractions such as ethane, propane, and butane can be used as feedstock to refineries; meanwhile, the heavier hydrocarbons can be employed as gasoline-blending stock [27]. Its production depends on heavy hydrocarbon content of the natural gas to be processed [28]. The extraction of ethane and NGL from natural gas is generally based on some of the following alternatives: (i) external refrigeration (ER), (ii) turboexpansion (TE), (iii) Joule-Thompson expansion, and (iv) absorption [29]. Refrigeration systems for NGL recovery use either propane or butane as refrigerants. In some applications, mixed refrigerants and cascade refrigeration cycles have been applied [30, 31].

In all previous studies, only some single subsystem was investigated, e.g., gas sweeting, gas dehydration, or NGL recovery subsystem. In this study, a comprehensive gas processing plant (CGPP) coupling sweetening, dehydration, NGL recovery, and compression subsystems has been simultaneously designed, modeled, and optimized based on field data, which has never been reported before. This merit echoes the application reality that all subsystems have to be considered simultaneously to comprehensively investigate operating conditions such as pressure, temperature, and flow rate that might affect each subsystem. Meanwhile, the integrated system could also enable the equipment sizing for four subsystems to be done simultaneously.

The simulation result indicates that the desired rate of return of the developed CGPP process is about 20 % per year; and the payback period will be 1.5 years. So, this study provides more valuable insights and solid foundation than ever for the entire natural gas processing from the viewpoint of the large-scale process system integration, modeling, and optimization. It will have a great potential to benefit future industrial design, operating, as well as budgeting and cost estimation.

2 Methodological Framework

The developed methodology framework contains four major stages of work as illustrated in Fig. 1. In the first stage, rigorous modeling and simulation will be conducted for the developed CGPP process. In this paper, Aspen HYSYS version 10 is employed to generate the entire process simulation model based on field data. In the second stage, the performance of all distillation columns, which are key units of the developed CGPP process, will be thoroughly investigated via sensitivity studies. Based on these studies, optimum operating conditions for all distillation columns could be identified. Sensitivity studies for three subsystems are performed.

- For the gas sweeting subsystem, the performance of acid gas absorption efficiency and solvent diethanol amine (DEA) loss in the absorption tower with respect to different operating pressure, temperature, and flow rate will be investigated. Meanwhile, the reboiler duty and solvent (DEA) loss of the regeneration tower with respect to its operating temperature will also be assessed.
- For the gas dehydration subsystem, the performance of water absorption efficiency and solvent loss (i.e., TEG loss) of the absorption tower with respect to different pressure, temperature, and flow will be investigated. Also, the performance of reboiler duty and solvent (TEG) loss in the regeneration tower with respect to its different operating temperature will also be analyzed.
- For the NGL recovery subsystem, the demethanizer tower performance with respect to its operating pressure and temperature will be examined. Based on the sensitivity study results, the optimal design and operating parameters for all distillation columns will be identified.

Next, sizing for major equipment of the developed CGPP process will be performed in the third stage based on updated simulation results. In the last stage, economic evaluations with Aspen process economic analyzer will be conducted to calculate the expected capital, installation, and operating expenditures for the developed CGPP process. Certainly, if the simulation results of each step are not satisfying, troubleshooting for all the possible upper stages of works will be performed; such a working procedure will be iterated until the final satisfying solution of the CGPP is obtained. Note that major tasks for each stage of work are also listed in Fig. 1. In the following context, more detailed descriptions for each stage of work are given.

3 CGPP Process Development and Modeling

Aspen HYSYS (version 10) is employed to generate the entire process simulation model. The PENG-ROB equation-of-state is used as the thermodynamic property method for simulation because it is recommended for gas processing, refinery, and petrochemical applications. The acid gas equation-of-state is taken for the gas sweeting subsystem and the glycol equation-of-state for the gas dehydration subsystem. The gas plant flow rate and composition particularly depend on the plant capacity and the reservoir composition. The typical gas plant flow rate

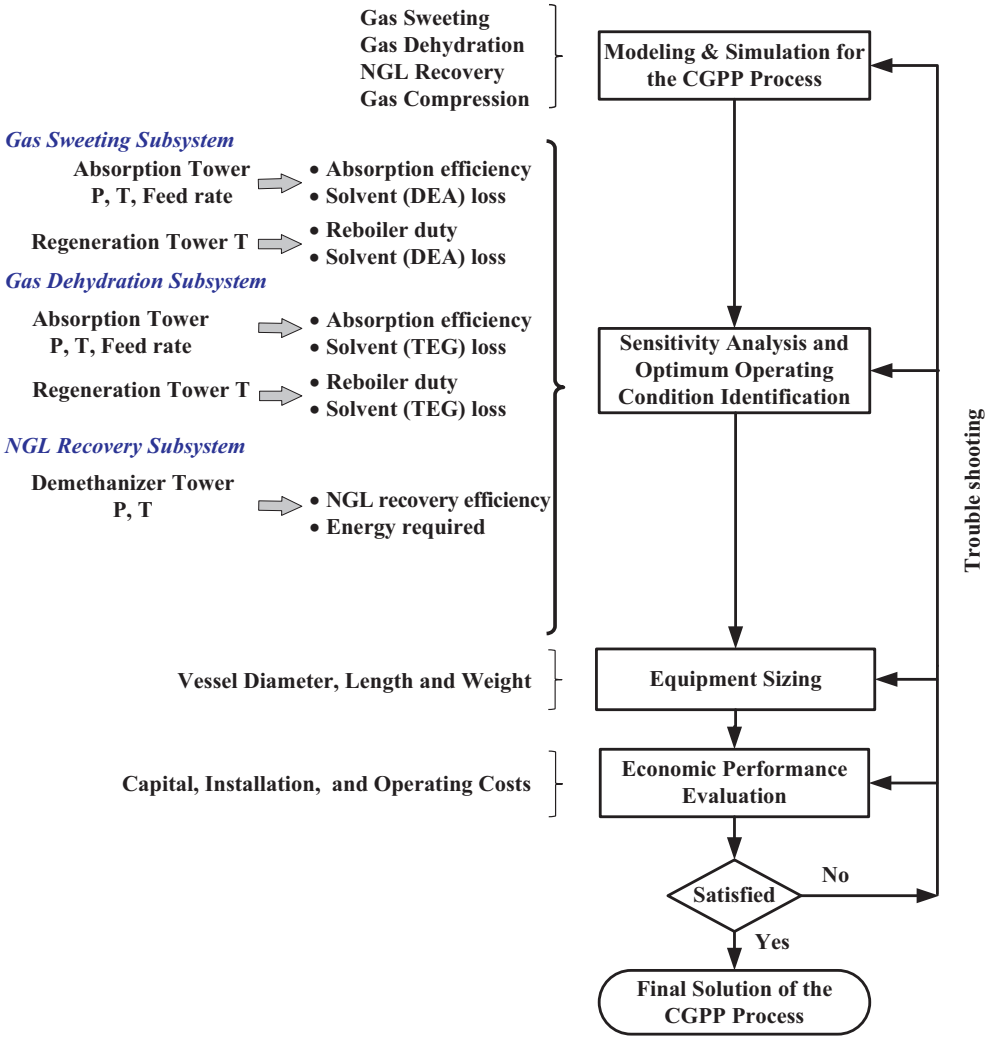

Figure 1. Methodological framework.

varies from 20 000 to 1.2 million m^3h^{-1}, and the methane composition can change from 0.4 % to 0.95 %. The typical model composition of natural gas, also used in this study, is presented in Tab. 1.

The inlet feed gas contains 0.1 % nitrogen, 2.87 % CO_2, 1.57 % H_2S, 75.2 % methane, 9.7 % ethane, 6.4 % propane, 1.06 % isobutane, 0.65 % *n*-butane, 0.3 % isopentane, 0.15 % *n*-pentane, and 1.87 % H_2O. The big picture of the developed CGPP HYSYS model is given in Fig. 2.

3.1 Sweetening Subsystem and Simulation Results

At the beginning of the CGPP process, 300 300 m^3h^{-1} of natural gas (Inlet Gas) enters into a feed-water knockout drum (FWKO). The purpose of this unit is to remove water/condensates from the gas stream. After that, all of the gas (Sour Gas) flows into the acid gas removal column (C-201). The gas stream then reacts with DEA in the absorption column (C-201). The amount of sweet gas coming out from top of the column (Sweet Gas) is 281 800 m^3h^{-1} while the DEA fed to the column (DEA Feed) is 425 m^3h^{-1}. The rich amine effluent from the bottom of the absorption column (Rich DEA) is 456 m^3h^{-1}. This Rich DEA stream then goes to the regeneration column, where the absorbed acid gases will be removed. The flow rate of acid gas leaving the regeneration column (C-206) is 17 820 m^3h^{-1} (Acid Gas). The flow rate of regenerated lean DEA (C-206B) leaving from the bottom of the regeneration column (C-206) is 422 m^3h^{-1}. After sweetening, the mole percentage of CO_2 and H_2S from 2.87 and 1.57 in the Sour Gas stream becomes 0.01 and 0 in the sweet gas (Sweet Gas), respectively. Hence, the gas stream is almost free of acid gases and the removal efficiencies of 99.7 % for CO_2 and 100 % for H_2S are achieved.

3.2 Dehydration Subsystem and Simulation Results

Fig. 2 also presents the process flow diagram for the natural gas dehydration subsystem. The sweet gas (Sweet Gas) of 281 800 m^3h^{-1} coming from the top of acid gas removal unit (represented as To Dehydration) enters the bottom of dehydration absorber column C-103. The liquid desiccant of TEG (TEG Feed) flows downward from the top of this column. The

Table 1. Operating conditions and composition of inlet gas, acid gas, NGL, and sales gas.

Parameter	Inlet gas	Acid gas	NGL	Sales gas
Flow [m^3h^{-1}]	300 300	17 820	50 850	230 300
Pressure [kPa]	8273	190	1380	6200
Temperature [°C]	30	82	25	30
Nitrogen [mol %]	0.10	0.0	0.0	0.001
CO_2 [mol %]	2.87	46.13	0.22	0.0
H_2S [mol %]	1.57	26.20	0.0	0.0
Methane [mol %]	75.20	0.19	1.75	97.27
Ethane [mol %]	9.70	0.02	46.31	2.40
Propane [mol %]	6.40	0.01	37.31	0.09
i-Butane [mol %]	1.05	0.0	6.14	0.0
n-Butane [mol %]	0.65	0.0	3.83	0.0
i-Pentane [mol %]	0.30	0.0	1.74	0.0
n-Pentane [mol %]	0.15	0.0	0.88	0.0
n-Hexane [mol %]	0.08	0.0	0.47	0.0
n-Heptane [mol %]	0.06	0.0	0.35	0.0
H_2O	1.87	27.39	0.0	0.0

(Dry Gas) of 281 100 m^3h^{-1} from top of C-103 is then passed through the next unit for further treatment which is represent as (To NGL Recovery Unit). The amount of vent gas (C107D) coming out of the dehydration regeneration unit (C-107) is 650 m^3h^{-1}, which mainly consists of water vapor (about 98.7 %). The lean TEG (C107B) coming out from the bottom of the regeneration unit (C-107) is 14.7 m^3h^{-1} and the makeup (TEG) flow rate is 0.0013 m^3h^{-1} for the entire dehydration subsystem. The amount of water in the inlet stream (To Dehydration) to the absorber column (C-103) is about 0.08 mole % and this amount is further reduced to 0.0 mole % after dehydration.

3.3 NGL Recovery and Compression Subsystems and Simulation Results

After dehydration, the treated gas will get into the gas subcooled process (GSP) by turboexpansion. Fig. 2 gives the schematic diagram of the NGL recovery process. The feed in this NGL recovery subsystem (To NGL Recovery Unit) is firstly cooled by the heat exchangers HX-302, HX-301, and HX-303. The precooled feed is sent to a separator (V-304) where the liquid is separated from the gas stream. A portion of the separated gas is further cooled by the heat exchanger HX-310 with the effluent directed to the demethanizer column (C-307). The other portion of the separated gas from V-304 is expanded in a turboexpander (K-305) and sent to the demethanizer via a preparator of V-306. Meanwhile, the liquid stream leaving the separator (V-304) enters the demethanizer at a lower stage. The demethanizer overhead is termed as the residue gas (C307V), which is directed to HX310 for heated up. After that, part of the power required to recompress the residue gas stream by the compressor (K-311) is provided by the turboexpander (K-305). Another compressor (K-312) is still needed to bring the final output (Sales Gas) pressure up to 6205 kPa. The demethanizer bottom stream (NGL) contains all the remaining C2+ hydrocarbons.

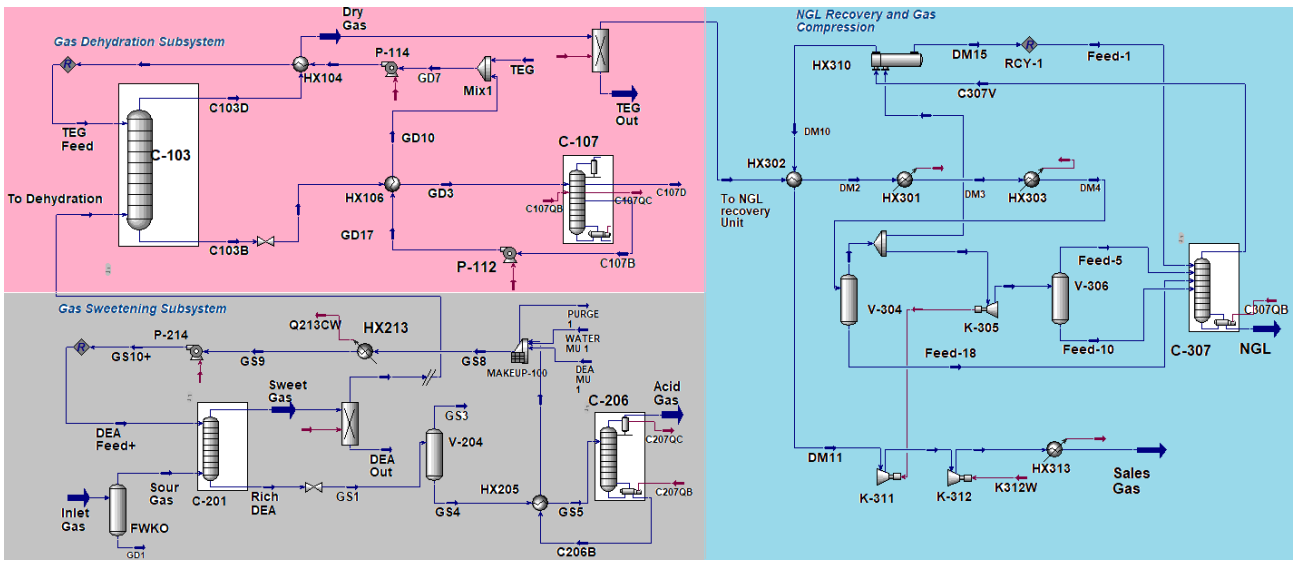

Figure 2. Flow diagram of the developed CGPP process.

4 Sensitivity Analysis

As distillation columns play critical roles in the performance of the developed CGPP process, sensitivity analyses are performed for those columns in order to identify their optimal operating conditions. The first step of the sensitivity analysis is to determine independent variables in the CGPP process to distinguish the effect of such variables on the column performance. The independent variables can be divided into two categories. The first category mainly includes operational parameters of the DEA and TEG absorption tower pressures, temperatures, and solvent (DEA and TEG) flow rates, as well as reboiler temperatures of regeneration towers. The second category involves operational parameters of natural gas such as inlet gas flow rate and temperature.

Based on the independent variables, important dependent variables which strongly affect the CGPP process performance, such as H_2O and CO_2 absorption efficiency from the natural gas, the makeup flow rate of DEA and TEG, the amount of solvent losses, as well as the amount of energy consumption represented by reboiler duties in gas sweetening and dehydration subsystems, are identified. In both gas sweeting and dehydration subsystems, the CO_2, H_2S, and H_2O absorption performances increase with higher absorption column pressure. Though a higher pressure would bring higher capital cost of column, the main goal is to remove the CO_2, H_2S, and H_2O from the sales gas to meet the customer specification. If one cannot remove the CO_2, H_2S, and H_2O from the sales gas, it will not meet the ultimate goal. Note that the associated capital cost with high pressure factor was not considered in this study.

4.1 Sensitivity Analysis for the Gas Sweetening Subsystem

Acid gas absorption was carried out through an absorption column (C-201), where a lean DEA solution flows in countercurrent to the natural gas stream as displayed in Fig. 2. The simulated influences on acid gas absorption and DEA loss against the absorption pressure and temperature are illustrated in Figs. 3 and 4, respectively. According to the Fig. 3, the absorption column (C-201) pressure could be ranged from 4825 to 8 275 kPa. The absorption performance increases with higher pressure. Meanwhile, the variation of amine loss with absorption pressure is very small, which can be negligible. Thus, 8275 kPa is the best absorption pressure as the maximum acid gas absorption could be achieved at this pressure while the DEA loss rate was almost unchanged.

From Fig. 4, the acid gas absorption performance has no significant influence with the temperature change at the absorption column (C-201). However, the increment of the

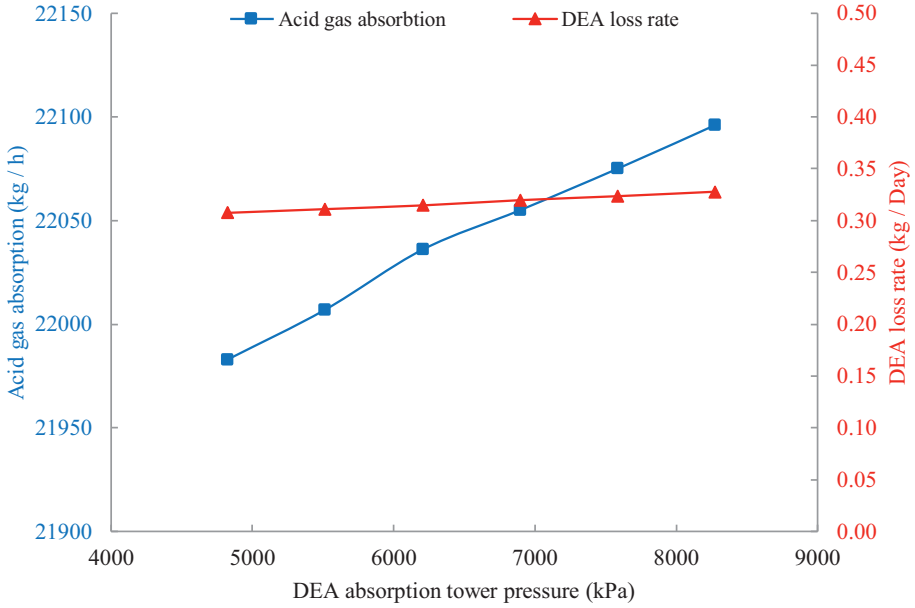

Figure 3. Effects of DEA absorption pressure on acid gas absorption and DEA loss.

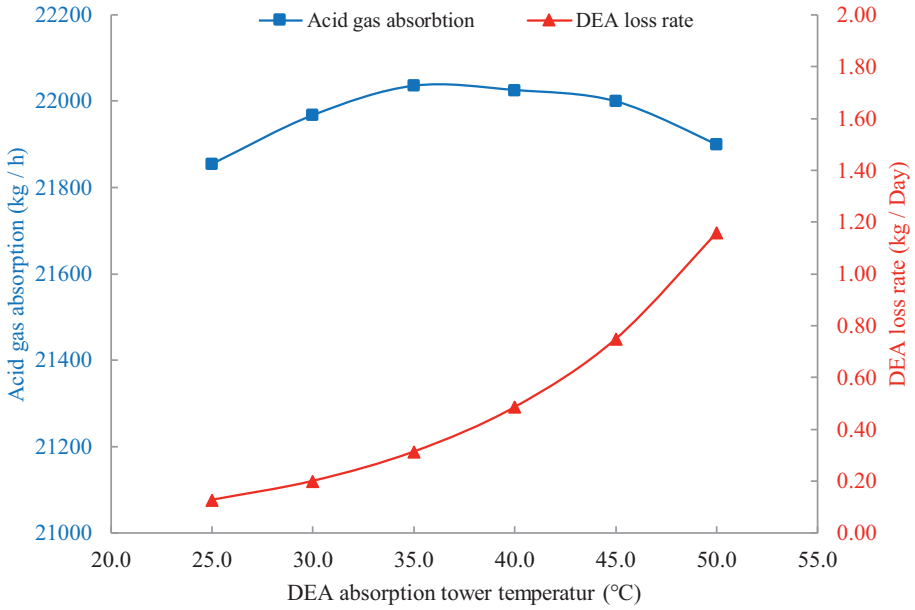

Figure 4. Effects of DEA absorption temperature on acid gas absorption and DEA loss.

DEA absorption tower (C-201) temperature will cause an accelerated DEA loss in the regeneration stripper (C-206). Thus, 30 °C is set as the preferred operating temperature at C-201 to trade off between the acid gas absorption performance and the DEA loss rate.

Based on simulation, Fig. S2 in the Supplementary Information reveals that as the DEA flowrate increases, the total heat duty, which represents the major energy consumption in the gas sweetening subsystem, also rises. This is because more energy will be required for solvent purification and cooling at a higher solvent flow rate. Fig. S2 also demonstrates the effect of DEA circulation rate on the acid gas absorption performance. It shows that the acid gas absorption rate will rise gradually versus the increase of solvent circulation rate. However, after the solvent circulation rate overpasses 446 100 kg h^{-1}, the acid gas absorption rate will not increase much while the reboiler duty of the regeneration stripper (C-206) still rises significantly. Therefore, 446 100 kg h^{-1} is selected as the preferred solvent circulation rate for the absorption column (C-201).

Note that the DEA loss with the acid gas from the top of regenerator (C-206) and reboiler duty depend on the regenerator reboiler temperature. Fig. S3 in the Supplementary Information illustrates the variation of the DEA loss rate with respect to the reboiler temperature of the regenerator C-206. The total reboiler heat duty has two functionalities, namely, to provide the sensible heat for heating the rich amine from feed temperature to its reboiler temperature and to provide the latent heat to vaporize the absorbed acid gas. In fact, under a fixed feed condition, the variation of the regenerator reboiler heat duty is predominantly due to the latent heat of the acid gas vaporization. The reboiler duty will increase with the increment of the reboiler temperature as indicated in Fig. S3. In the meantime, simulation indicates that the DEA loss exhibits only minor changes with reboiler temperature changes. To maintain 110 °C temperature at the regenerator (C-206) reboiler is best.

4.2 Sensitivity Analysis for the Dehydration Subsystem

Water absorption was carried out through a column (C-103) where a lean TEG solution flows in countercurrent to the natural gas stream shown in Fig. 2. The simulated influence of absorption pressure and temperature is illustrated in Fig. 5 and 6. According to Fig. 5, the pressure for maximum absorption ranges from 4825 to 8275 kPa. Absorption performance increases with higher absorption column (C-103) pressure. Moreover, the TEG absorption tower pressure reduction causes

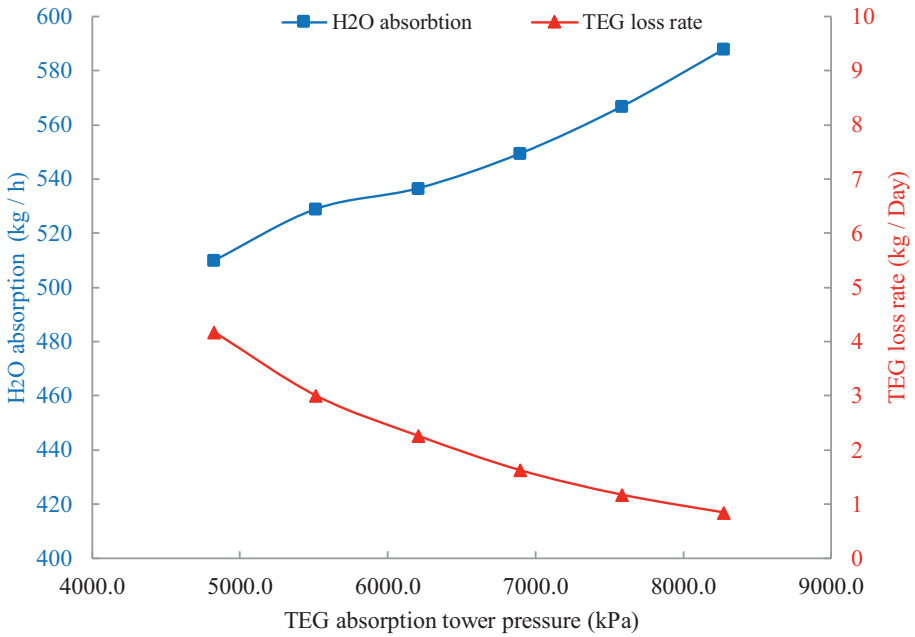

Figure 5. Effects of TEG absorption pressure on water absorption and TEG loss.

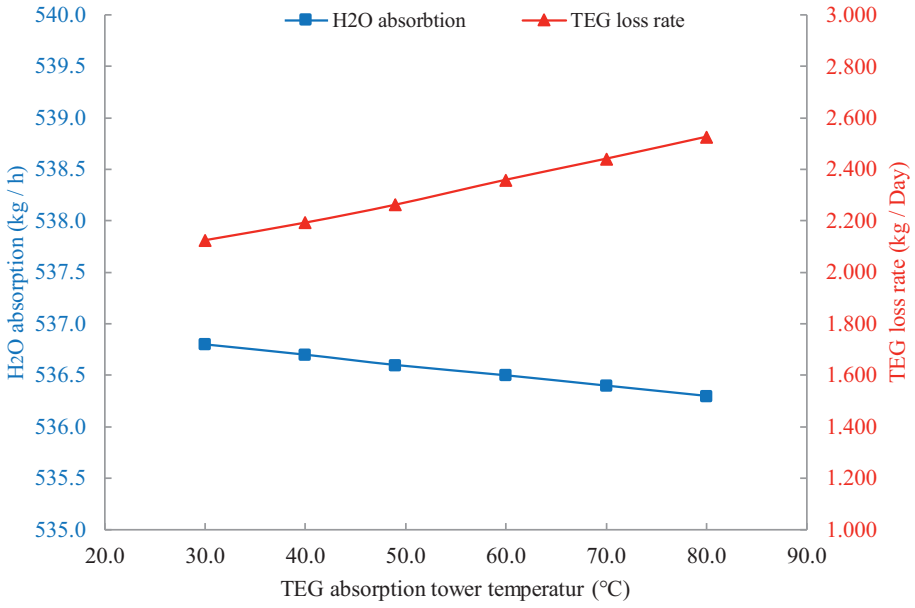

Figure 6. Effects of TEG absorption temperature on water absorption and TEG loss.

more evaporation (TEG losses) in the stripper, which means more glycol makeup is needed. Variation of glycol loss with absorption pressure is illustrated in Fig. 5. Consequently, 8275 kPa is thought to be the best in terms of balancing H_2O absorption and TEG loss.

On the other hand, absorption has no significant influence with the changing of gas temperature at the absorption column (C-103) which is illustrated in Fig. 6. Moreover, the TEG absorption tower (C-103) temperature increase causes more evaporation in the regeneration stripper (C-107), so TEG losses rise gradually.

In order to minimize the water content of the outlet dry gas, the glycol circulation rate needs to be increased. Fig. S4 in the Supplementary Information reveals that as the TEG flow rate rises, the total heat duty or energy consumption in dehydration and regeneration processes increases. The main reason is that more energy is required for gas cooling and solvent purification at higher solvent flow rate. This figure also displays the effect of TEG circulation rate on the water absorption from the sweet gas. The sensitivity of the water absorption to the rate of glycol increases gradually by raising the glycol rate. However, after a glycol rate of 16 600 kg h^{-1}, the water absorption rate is not increased significantly whereas the boiler duty rises distinctly. Increasing the TEG circulation rate will boost the operating costs. Thus, 16 600 kg h^{-1} is considered as the minimum feasible rate for glycol circulation rate for the optimization of the absorption column (C-103). Solvent (i.e., TEG) loss at different solvent flow rates has no significant influence.

Some parameters such as TEG loss in the top of the regenerator (C-107) and reboiler duty depend on the regenerator temperature and were evaluated as well. The TEG loss becomes larger because the mass flow rate of the stripping vapor generated by the reboiler increases with regenerator temperature. Fig. S5 in the Supplementary Information illustrates the variation of the TEG loss with regenerator (C-107) temperature.

The total reboiler heat duty has two functionalities, i.e., to provide the sensible heat for heating the rich glycol from feed temperature to reboiler temperature and to provide the latent heat to vaporize water. In fact, under fixed feed condition, the variation of the regenerator heat duty is predominantly due to the latent heat of water vaporization. Higher reboiler duty is achieved by increasing the reboiler temperature as it can be seen in Fig. S5. To maintain the 210 °C temperature at the regenerator (C-107) reboiler is the best as it absorbs the H_2O sufficiently and leads to minimum reboiler duty and TEG loss. A further increase of the reboiler temperature does not affect the H_2O absorption whereas it raises the reboiler duty and thus the energy loss significantly.

4.3 Sensitivity Analysis for NGL Recovery and Compression Subsystems

In the NGL recovery subsystem, the critical step is to produce the desired liquid product by means of a fractionation column. The column in this study is called demethanizer column (see C-307 in Fig. 2), which separates methane and other more volatile components at the top of the column from ethane and less volatile components in the purified gas stream. The performance of the NGL recovery process is highly dependent on the operating pressure and temperature of the demethanizer column. A demethanizer is operated at medium to low pressure to separate the lighter components [31]. As suggested by Chebbi [32], the typical range of demethanizer operating pressure should be 690–3100 kPa. Though tuning the reflux ratio is also responsible for NGL recovery, the key design variable for a demethanizer is the operating pressure of the column, as changing column operating pressure significantly affects different important operating conditions such as relative volatilities, vapor loads, and temperature profiles inside the columns.

Meanwhile, as the ethane boiling point is near –90 °C, the investigated demethanizer operating temperature should be around –90 °C. The three consecutive heat exchangers, i.e., HX-301, HX-302, and HX-303, are to reduce the gas temperature. Also, the sudden pressure drop in separator V-304 and the use of turbo expander K-305 decrease the gas temperature significantly. Thus, the sensitivity study for the demethanizer performance covers the pressure varieties from 690–3100 kPa and the temperature variations from to –70 to –100 °C. Fig. 7 demonstrates the simultaneous effect of demethanizer pressure and temperature on NGL recovery efficiency. It indicates that a higher NGL recovery efficiency will be obtained at both lower demethanizer pressure and temperature.

Fig. 8 illustrates the simultaneous effect of demethanizer pressure and temperature on the energy consumption including the demethanizer reboiler duty (see C-307 in Fig. 2) and the compression energy (see K-312 in Fig. 2) required in the downstream compression subsystem. Note that K-311 is driven by K-305, which belongs to the internal energy recovery. From

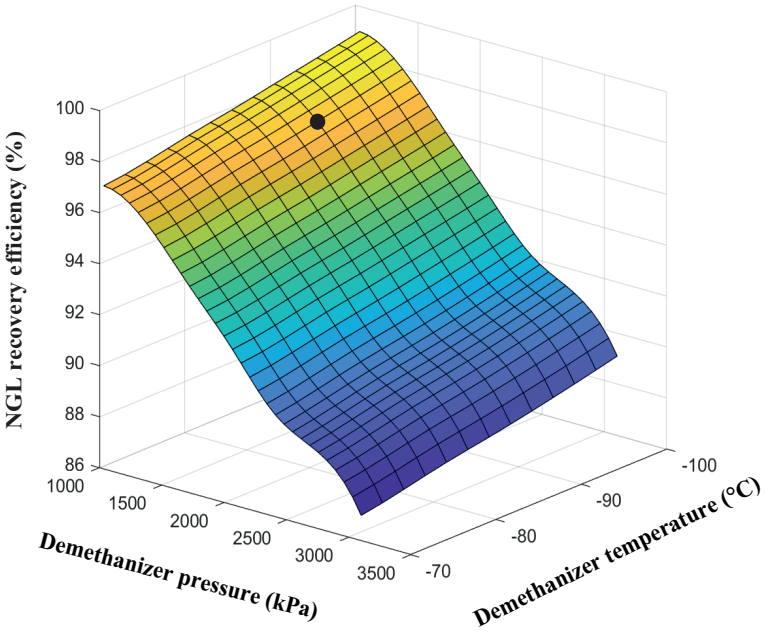

Figure 7. Effect of demethanizer pressure and temperature on NGL recovery efficiency.

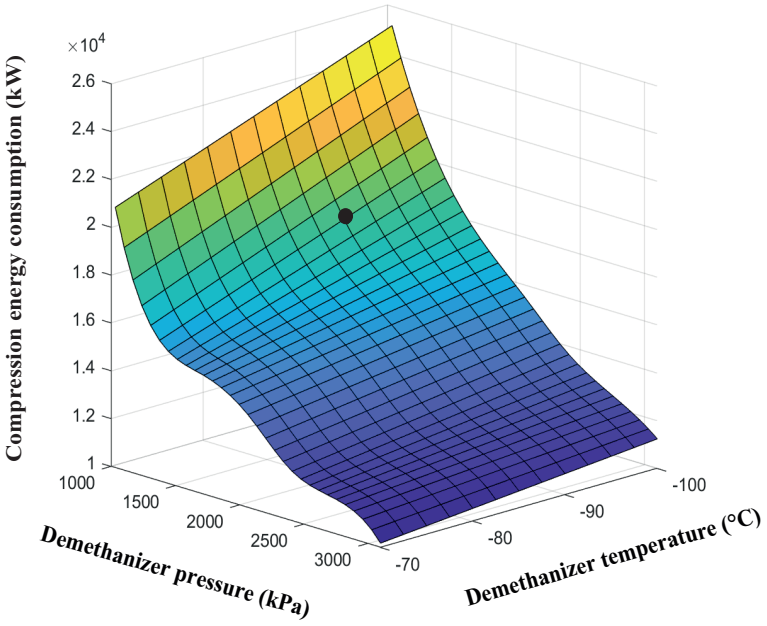

Figure 8. Effect of demethanizer pressure and temperature on energy consumption in NGL recovery and compression subsystems.

Fig. 2 it is obvious that the higher compression energy will be required at a lower demethanizer pressure. This is because at a low demethanizer pressure the top outlet pressure of the residue gas (C-307V) will be also low, which requires the downstream of K-312 (see Fig. 2) to spend more energy to gain the specified pressure for the sales gas.

Meanwhile, the energy consumption in NGL recovery and compression subsystems will become higher at a lower demethanizer operating temperature, which is because at a lower demethanizer temperature the reboiler of C-307 needs more energy for heating the bottom liquid. As indicated in Fig. 8, the higher energy consumption will result from both lower demethanizer pressure and temperature. As the NGL recovery efficiency is better to be higher than 96 % and the required energy will be significantly high when NGL recovery efficiency reaches 99 %, the selected operating pressure and temperature for the demethanizer are 1380 kPa and –90 °C, respectively. Generally, the settings are to balance the NGL recovery and energy consumption. Under these operating conditions, the NGL recovery efficiency is 97.3 %.

5 Economic Performance Evaluation

The economic evaluation aims to estimate various costs, product sales, and the payback period to invest such a new CGPP project. It is based on the process design and equipment sizing information, which is presented in the Supplementary Information with detailed description. The project cost includes total capital cost and operating costs of the entire process. The total capital cost involves equipment cost and installation cost of all units. The utility cost considers electricity, steam, cooling water, high-pressure steam, and low-pressure steam. The operating cost comprises the total raw materials (i.e., feed cost and chemical consumption), unit operation, and total utility costs. The costs and installed weights for major equipment are summarized in Tab. 2.

The utility cost of the CGPP process is presented in Tab. 3. The total cost of the gas processing plant is given in Tab. 4. It shows both capital and operating cost as well as the total product sale. The total product sale includes 230 300 m^3h^{-1} natural gas sales and 188.2 m^3h^{-1} NGL. The crude oil/gas market changes every single day. In the last five years, it varied from 20 to 100 USD per barrel. The natural gas price also varied from 2 to 6 USD for per thousand cubic feet. Considering the natural gas sales price of 5 USD per thousand cubic feet and the NGL sales price of 60 USD per barrel which are typical prices within these ranges, the payback period will be around 1.5 years.

6 Conclusions

The aim is to develop and optimize a comprehensive gas processing plant (CGPP) for sales gas and NGL productions, which seldom has been systematically studied as an integrated system from the previous studies. The CGPP process consists of sweetening, dehydration, NGL recovery, and compression subsystems. The development included four major stages of work: (i) CGPP process development with Aspen HYSYS simulator; (ii) sensitivity studies for all distillation columns involved in the CGPP process to optimize their performances; (iii) sizing of major equipment of the CGPP; and (iv) economic evaluations with Aspen process economic analyzer to calculate the expected capital and operating expenditures for the developed CGPP process.

Considering the natural gas sales price of 5 USD per thousand cubic feet and an NGL sales price of 60 USD per barrel, the payback period of the entire gas processing plant will be 1.5 years. This study provides valuable insights of natural gas monetization from the viewpoint of the large-scale process system integration, modeling, and optimization.

Supporting Information

Supporting Information for this article can be found under DOI: https://doi.org/10.1002/ceat.202000216.

Acknowledgment

This work is supported by The Center for Midstream Management and Science (CMMS), Graduate Student Scholarship, and Anita Riddle Faculty Fellowship from Lamar University in Beaumont, TX, USA.

The authors have declared no conflict of interest.

Table 2. Summary of major equipment cost and weight.

Unit index	Equipment cost [USD]	Installed cost [USD]	Equipment weight [lbs]	Installed weight [lbs]
HX301	2 167 900	3 408 900	758 500	1 073 310
V-306	32 100	152 000	9500	24 894
FWKO	99 700	223 700	46 600	68 231
C-107	46 700	288 300	8570	46 260
K-312	2 006 200	2 354 400	59 700	125 751
HX106	13 000	77 800	2300	13 486
HX104	36 900	124 200	10 300	30 140
HX205	153 800	290 100	59 500	93 611
K-311	1 028 300	1 251 300	22 100	55 404
HX313	1 192 500	1 535 300	420 900	512 260
C-201	381 600	619 100	177 400	214 264
P-112	5000	39 500	230	4968
C-206	500 100	1 112 600	167 600	305 027
HX302	89 300	228 400	27 200	62 811
HX303	4 087 100	6 235 300	1 422 900	1 978 314
P-214	276 100	435 200	13 700	49 116
C-103	254 000	473 300	104 100	138 226
C-307	809 700	1 340 000	341 400	444 433
K-305	543 400	694 900	19 900	27 988
V-304	139 000	316 000	70 700	102 237
HX310	336 100	632 100	91 000	159 873
HX213	2 416 700	3 883 100	991 200	1 300 596
P-114	64 500	106 900	3900	9607
V-204	81 200	239 500	30 200	56 736

Abbreviations

CGPP comprehensive gas processing plant
DEA diethanol amine
NGL natural gas liquid
TEG triethylene glycol

Table 3. Utility consumption and cost of the developed CGPP process.

Items	Consumption rate	Unit price	Cost per hour (USD)
Electricity	10 177.21 kW h^{-1}	0.06 \$ kW^{-1}	586.20
Cooling water	0.094 MMGAL h^{-1}	120 \$ $MMGAL^{-1}$	11.25
Steam at 100 psig	120.78 klb h^{-1}	8.14 \$ klb^{-1}	983.08
Low-pressure steam	167 348 340 BTU h^{-1}	1.26×10^{-6} \$ BTU^{-1}	211.95

Table 4. Overall economic evaluation results for the developed CGPP process.

Items	Cost
Total capital cost [USD]	41 884 400
Total operating cost [USD a^{-1}]	421 211 000
Total raw materials cost [USD a^{-1}]	371 854 000
Total product sales [USD a^{-1}]	454 092 000
Total utilities cost [USD a^{-1}]	15 713 000
Desired rate of return [% a^{-1}]	20
Payback period [a]	1.5
Equipment cost [USD]	16 760 900
Total installed cost [USD]	26 061 900

References

[1] W. L. Luyben, *Ind. Eng. Chem. Res.* **2013**, *52*, 11626–11638.
[2] D. Galatro, F. M. Cordero, *Nat. Gas Sci. Eng.* **2014**, *18*, 112–119.
[3] M. M. Ghiasi et al., *Nat. Gas Sci. Eng.* **2014**, *17*, 26–32.
[4] T. E. Rufford et al., *Pet. Sci. Eng.* **2012**, *94–95*, 123–154.
[5] M. D. Rincon et al., *Nat. Gas Sci. Eng.* **2016**, *29*, 264–274.
[6] A. R. Sayed et al., *Chem. Eng. Res. Des.* **2017**, *124*, 114–123.
[7] F. T. Okimoto, G. Gadeholt, *Best practices Guide Gas sweetening Technology*, Shell international exploration and production, Rijswijk **1998**, BV 55.
[8] S. Mokhatab, J. Y. Mak, J. V. Valappil, D. A. Wood, *Handbook of Liquefied Natural Gas*, Elsevier, Amsterdam **2014**.
[9] N. Rodriguez et al., *Chem. Eng. Res. Des.* **2011**, *89*, 1763–1773.
[10] M. L. Spears, K. M. Hagan, J. Bullin, C. J. Michalik, Converting to DEA/MDEA Mix Ups Sweetening Capacity, *Oil Gas J.* **1996**, 63–67.
[11] J. Polasek, J. Bullin, Selecting Amines for Sweetening Units, *Energ. Prog.* **1994**, *4* (*3*), 146–149.
[12] A. N. Rouzbahani et al., *Nat. Gas Sci. Eng.* **2014**, *21*, 159–169.
[13] M. Netusil, P. Ditl, *J. Nat. Gas Chem.* **2011**, *20 (5)*, 471–476.
[14] C. A. Scholes et al., *Fuel* **2012**, *96*, 15–28.
[15] H. A. Farag et al., *Alex. Eng. J.* **2011**, *50*, 431–439.
[16] H. Lin et al., *J. Memb. Sci.* **2012**, *413–414*, 70–81.
[17] M. Neagu, D. L. Cursaru, *Nat. Gas Sci. Eng.* **2017**, *37*, 327–340.

[18] A. Karimi, M. A. Abdi, *Chem. Eng. Process.* **2009**, *48*, 560–568.
[19] C. Wen et al., *Chem. Eng. Process.* **2011**, *50*, 644–649.
[20] P. Wieninger, *Proc. Laurance Reid Gas Conditioning Conf.* **1991**, 23–59.
[21] R. L. Pearce et al., *Hydrocarbon Process.* **1972**, *51 (12)*, 79–81.
[22] K. Paymooni et al., *Energy Fuels* **2011**, *25*, 5126–5137.
[23] R. S. Smith, *Proc. Laurance Reid Gas Conditioning Conf.* **1993**, 101–114.
[24] M. R. Rahimpour et al., *J. Nat. Gas. Sci. Eng.* **2013a**, *12*, 1–12.
[25] M. R. Rahimpour et al., *J. Nat. Gas. Sci. Eng.* **2013b**, *15*, 118–126.
[26] M. Mehrpooya et al., *J. Nat. Gas Sci. Eng.* **2017**, *42*, 262–270.
[27] M. S. Khan et al., *Chem. Eng. Process.* **2014**, *82*, 54–64.
[28] M. Getu et al., *Comput. Aided Chem. Eng.* **2012**, *31*, 405–409.
[29] M. Mazumder, Q. Xu, in *Natural Gas Processing from Midstream to Downstream* (Eds: N. O. Elbashir, M. M. El-Halwagi, I. G. Economou, K. R. Hall), John Wiley & Sons, New York **2018**, Vol. 2, 235–257.
[30] M. Mehrpooya et al., *Int. J. Energy Res.* **2009**, *33*, 960–977.
[31] M. Mehrpooya et al., *Iran J. Chem. Chem. Eng.* **2012**, *31 (3)*, 97–109.
[32] R. Chebbi et al., *Chem. Eng. Res. Des.* **2010**, *8 (8)*, 779–787.

